



# Tsunami Wave Generation by Solid and Deformable Landslides

Gangfeng Ma<sup>1</sup> (gma@odu.edu), Kirby J.T.<sup>2</sup> (kirby@udel.edu), Shi F.<sup>2</sup> (fyshi@udel.edu), Grilli S.T.<sup>3</sup> (grilli@oce.uri.edu)

1. Department of Civil and Environmental Engineering, Old Dominion University, Norfolk, VA 23529
2. Center for Applied Coastal Research (CACR), University of Delaware, Newark, DE 19716
3. Department of Ocean Engineering, University of Rhode Island, Narragansett, RI 02882

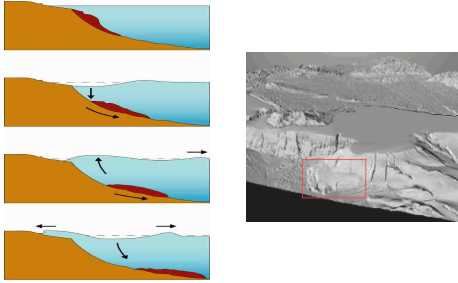


Fig.2 Comparisons of simulated and measured current velocities and sediment concentrations for case NOVAT at supercritical (x=0.3 m) and subcritical (x=0.8 m) regions. Both velocities and sediment concentrations are normalized by layer-averaged values.

The Non-Hydrostatic WAVE model NHWAVE (Ma et al., 2012) is employed to simulate both solid and deformable landslides. The governing equations include continuity and momentum equations in well-balanced conservative form:

$$\frac{\partial D}{\partial t} + \frac{\partial D u}{\partial x} + \frac{\partial D v}{\partial y} + \frac{\partial \omega}{\partial \sigma} = 0$$

$$\frac{\partial U}{\partial t} + \frac{\partial F}{\partial x} + \frac{\partial G}{\partial y} + \frac{\partial H}{\partial \sigma} = S_h + S_b + S_s + S_r$$

where  $D(x,y,t)=h(x,y,t)+\eta(x,y,t)$  is the total water depth,  $h(x,y,t)$  is the water depth, which is time dependent for solid landslide case,  $\eta$  is the free surface elevation,  $u$  and  $v$  are the horizontal velocities,  $\omega$  is the vertical velocity in surface and terrain following  $\sigma$  coordinate,  $S_h$ ,  $S_b$  and  $S_r$  are source terms related to hydrostatic pressure, dynamic pressure and turbulent diffusion, respectively.  $S_s$  is the baroclinic pressure gradient forcing, which is nil for homogeneous fluid (solid landslide problems in this study).

For solid landslide, the slide shape and behavior are prescribed based on a dynamic force balance involving weight, buoyancy, friction as well as hydrodynamic drag and inertia forces (Enet and Grilli, 2005). The slide motion is accounted for through a moving boundary condition (Ma et al., 2012):

$$w|_{z=-h} = -\frac{\partial h}{\partial t} - u \frac{\partial h}{\partial x} - v \frac{\partial h}{\partial y} \quad \frac{\partial p}{\partial \sigma}|_{z=-h} = \rho L \frac{\partial^2 h}{\partial t^2}$$

For deformable landslides, the slide is modeled as water-sediment mixture. Its motion is driven by the baroclinic pressure gradient forcing, which is introduced by the spatial variation of mixture density  $\rho_m$

$$\rho_m = (1 - C)\rho_0 + C\rho_s$$

where  $\rho_0=1000 \text{ kg/m}^3$  is the water density,  $\rho_s=2650 \text{ kg/m}^3$  is the sediment density,  $C$  is the sediment volume concentration, which is obtained by solving the convection-diffusion equation

$$\frac{\partial DC}{\partial t} + \frac{\partial DC u}{\partial x} + \frac{\partial DC v}{\partial y} + \frac{\partial (\omega - w_s)C}{\partial \sigma} = \frac{\partial}{\partial x} [D(\nu + \frac{v_s}{\sigma_s}) \frac{\partial C}{\partial x}] + \frac{\partial}{\partial y} [D(\nu + \frac{v_s}{\sigma_s}) \frac{\partial C}{\partial y}] + \frac{1}{D} \frac{\partial}{\partial \sigma} [(\nu + \frac{v_s}{\sigma_s}) \frac{\partial C}{\partial \sigma}]$$

in which  $w_s$  is the sediment settling velocity,  $\nu$  and  $\nu_s$  are molecular and turbulent diffusivity, respectively.  $k-\epsilon$  turbulence model is employed to calculate turbulent diffusivity.

## 1. Model validation

The model for stratified flows and sediment transport is validated by the laboratory measurements of turbidity currents reported by Garcia (1993). The experiments involve an internal hydraulic jump at the slope transition.

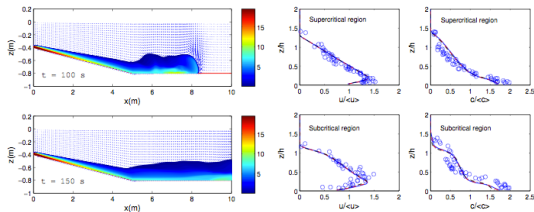


Fig.1 Distributions of simulated sediment concentrations for case NOVAT at t=100 s and 150 s, respectively.

Fig.2 Comparisons of simulated and measured current velocities and sediment concentrations for case DAPER at supercritical (x=0.3 m) and subcritical (x=0.8 m) regions. Both velocities and sediment concentrations are normalized by layer-averaged values.

## INTRODUCTION:

Submarine landslides can generate very large and energetic tsunami waves in the coastal areas. A variety of methods exist for simulating landslide tsunamis, ranging from methods based on solid body translation to methods based on slides having Newtonian or more rheologically complex liquid properties. However, benchmarks only exist for the solid slide case, and there has been little effort to compare and contrast the variety of surface wave responses.

Recently, we have performed extensive simulations of solid body landslides using a fully 3D non-hydrostatic model NHWAVE, developed by Ma et al. (2012). The original model solves the RANS equations for a homogeneous fluid in surface and terrain following coordinates. Solid body landslides are modeled utilizing the terrain following capability in an unsteady, moving boundary setting. More recently, the model has been extended to allow for the treatment of stratified flows. In this study, the version of the model for stratified flows is used to simulate wave generation by arbitrarily deformable landslides, which is modeled as water-sediment mixture. Its motion is driven by the baroclinic pressure gradient forcing, which is introduced by the spatial variation of mixture density. The resulting model is used together with the original moving boundary model to examine the relative tsunamigenic response to slides of equal initial geometry and density but having solid or liquid behavior at leading order.

The model for solid landslide is validated by the laboratory measurements of Enet and Grilli (2005). The slide geometry and along-slope displacement in the simulation follow the experiments.



Fig 3. General view of experimental setup: slope and landslide model (Enet and Grilli, 2005). The beach slope has an angle of 15°.

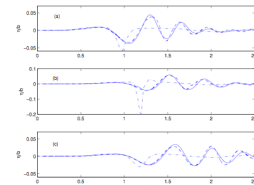


Fig 5. Comparisons between nonhydrostatic results (solid lines), hydrostatic results (dashed-dotted line) and experimental data (dashed line) for surface elevation at three wave gauges, which are located at (a)(1469, 350) mm; (b) (1929.0) mm and (c) (1929,500) mm.

## 2. Tsunami waves generated by a 2D deformable landslide

The model for stratified flows and sediment transport is employed to simulate tsunami wave generation by a 2D deformable landslide. The computational setup is shown in fig.7.

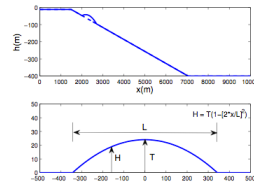


Fig 7. Sketch of the initial landslide, which is located at the gentle uniform slope with inclination angle  $\theta=4^\circ$ . The slide has a length of  $L=686 \text{ m}$  and a height of  $T=24 \text{ m}$ . The slide density is  $\rho_s=2000 \text{ kg/m}^3$ . The initial submergence depth is  $d=120 \text{ m}$ .

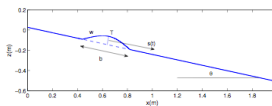


Fig 4. Vertical cross section of the numerical setup. The gaussian shape landslide model has length  $b=0.395 \text{ m}$ , width  $w=0.680 \text{ m}$  and thickness  $T=0.082 \text{ m}$  and is initially located at submergence depth  $d=61 \text{ mm}$ .

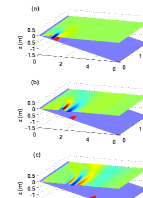


Fig 6. Snapshots of tsunami waves generated by solid landslide at (a)  $t=1.0 \text{ s}$ ; (b)  $t=2.0 \text{ s}$  and (c)  $t=3.0 \text{ s}$  after release of the sliding mass. The surface elevation is exaggerated by 5 times.

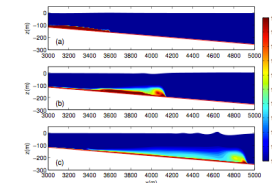


Fig 8. The motion of the landslide illustrated as the distributions of sediment concentration at (a)  $t=10 \text{ s}$ ; (b)  $t=50 \text{ s}$  and (c)  $t=100 \text{ s}$ . The landslide can be diluted and diffused during its movement.

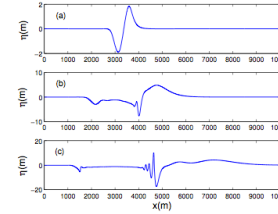


Fig 9. Tsunami waves generated by the deformable landslide at (a)  $t=10 \text{ s}$ ; (b)  $t=50 \text{ s}$  and (c)  $t=100 \text{ s}$ . Three wave trains are generated during the slide motion. The first one is led by a large wave crest, which propagates faster than the slide. The second one is led by a wave trough, which is directly forced by the landslide. The third wave train is a wave trough, propagating onshore. These wave trains are very dispersive.

## 3. Tsunami waves generated by 3D solid and deformable landslides

In this section, we examine the relative tsunamigenic response to 3D solid and deformable landslides of equal initial geometry and density. The landslides are defined using truncated hyperbolic secant function (Enet and Grilli, 2005) with length 686 m, width 343 m and height 24 m. The slides are initially located at 60 m water depth. The Slide density is 2000  $\text{kg/m}^3$ .

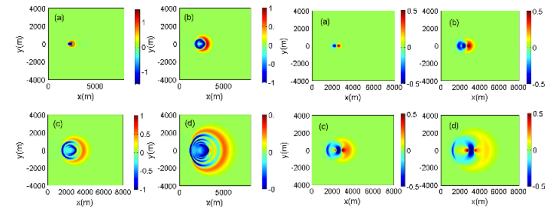


Fig 10. Snapshots of tsunami waves generated by 3D deformable landslide (left panels) and solid landslide (right panels) at (a)  $t=10 \text{ s}$ ; (b)  $t=30 \text{ s}$ ; (c)  $t=50 \text{ s}$  and (d)  $t=80 \text{ s}$ . Directional spreading of waves generated by deformable landslide is more significant. The wave energy is mainly concentrated on a narrow band from the dominant slide direction for the case of solid landslide.

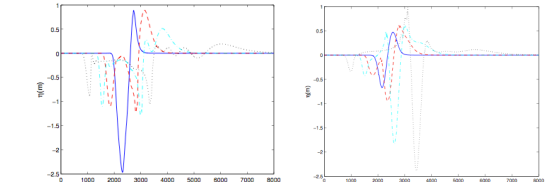


Fig 11. Free surface elevations in a vertical plane with  $y=0 \text{ m}$  generated by 3D deformable (left panel) and solid (right panel) landslides at  $t=10 \text{ s}$  (solid lines),  $30 \text{ s}$  (dashed lines),  $50 \text{ s}$  (dash-dotted lines) and  $100 \text{ s}$  (dotted lines). The deformable landslide can generate larger waves shortly after the release of the sliding mass. The solid landslide generates larger waves eventually.

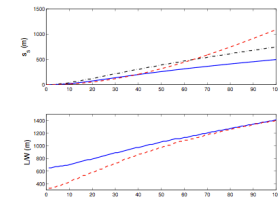


Fig 12. The along-slope displacement  $s_x$  of the deformable (solid lines) and solid (dashed line) landslides as well as the temporal variations of the length  $L$  and width  $W$  of the deformable landslide. The dashed-dotted line shows the displacement of the leading edge of the deformable landslide. At the beginning of the landslide ( $<40 \text{ s}$ ), the deformable landslide has larger velocity and acceleration, which lead to larger waves. The spreading effects in both along-slope and cross-slope directions are significant.

## References:

1. Enet F. and Grilli S.T., 2007, Experimental study of tsunami generation by three-dimensional rigid underwater landslide. *Journal of Waterway, Port, Coastal, and Ocean Engineering*, 133, 442-454
2. Garcia M.H., 1993, Hydraulic jumps in sediment-driven bottom currents, *Journal of Hydraulic Engineering*, 119, 1094-1117
3. Ma G., Shi F. and Kirby J.T., 2012, Shock-capturing non-hydrostatic model for fully dispersive surface wave processes, *Ocean Modelling*, 43-44, 22-35